Journal Pre-proofs

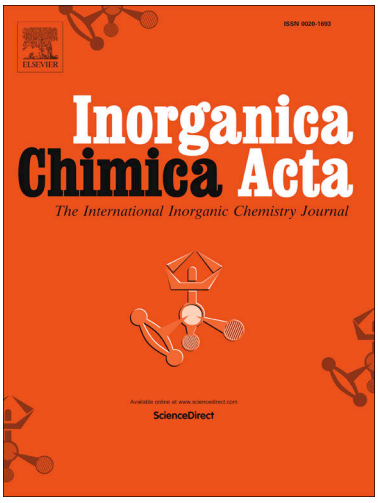

Research paper

Formation of a Lanthanoid Complex Shell on a Nanoparticulate Wax Core

Joo-Hyung Kim, Sujeethraj Koppolu, Eser Akturk, Eric Roth, Marc A. Walters

PII: S0020-1693(19)31874-2
DOI: https://doi.org/10.1016/j.ica.2020.119725
Reference: ICA 119725

To appear in: *Inorganica Chimica Acta*

Received Date: 1 December 2019
Revised Date: 24 April 2020
Accepted Date: 28 April 2020

Please cite this article as: J-H. Kim, S. Koppolu, E. Akturk, E. Roth, M.A. Walters, Formation of a Lanthanoid Complex Shell on a Nanoparticulate Wax Core, *Inorganica Chimica Acta* (2020), doi: https://doi.org/10.1016/j.ica.2020.119725

FORMATION OF A LANTHANOID COMPLEX SHELL ON A NANOPARTICULATE WAX CORE

Joo-Hyung Kim[a], Sujeethraj Koppolu[a], Eser Akturk[a], Eric Roth[b] and Marc A. Walters[a,*]

[a] *Department of Chemistry, New York University, New York, NY 10003, USA*
[b] *School of Medicine, Department of Radiology, New York University, New York, NY 10016, USA*

Address correspondence to:
Professor Marc A. Walters
NYU Dept. of Chemistry
100 Washington Square E.
marc.walters@nyu.edu
212-998-8477
fax: 212-995-4475
*

Abstract

Carboxylate-rich lanthanide complexes were employed as anion counterions to the cationic surfactant cethyltrimethylammonium (CTA) and assembled to form a shell around emulsifying wax nanoparticles. The anionic complexes consisted of lanthanide ions coordinated by the ligand DOTA-tetrahomoserine (DhS). In combination with CTA the complexes formed a surfactant system (CTA)[LnDhS] (Ln = Eu, Gd) with the nonpolar tail of CTA embedded in an emulsifying wax (EW) nanoparticle core. The DhS units were then crosslinked with divinylsulfone to form a shell around the EW core. Fluorescence and NMR data on the Eu complex were consistent with the formation of a stable polymeric shell around the wax core template. These results illustrate a general method that exploits electrostatic interactions leading to assembly of capsules around solid lipid nanoparticles. Preliminary relaxivity measurements were carried out on particles with Gd-containing shells.

Keywords: solid lipid nanoparticles; DOTA; cationic SLN; divinyl sulfone; hyperbranched; theranostics

1. Introduction

Bio-related coordination nanochemistry has a rich legacy in the development of diagnostic agents. This includes a large body of work on Gd^{3+} based T1 agents in, perfluorocarbons, liposomes, fullerenes, carbon nanotubes and polymer-based hybrid nanoparticles as well as related research on silver and gold nanoparticles.[1-4] Hybrid nanoparticles (NPs) are the subject of ongoing research as vehicles for simultaneous targeting, imaging, and drug delivery.[5] For a large fraction of hybrid NPs an organic superstructure is anchored on a noble metal core. A previous report from this laboratory featured silver NPs with surface anchored GdDTPA groups.[6] These particles served to concentrate gadolinium complexes into the molar range, (based on the volume of the particle) making them useful for MRI based molecular imaging. Until recently metal NP systems had been favored for their ease of formation and rich surface chemistry, where chemisorption on the metal surface is readily achieved with thiols, amines, and carboxyl links and others.[7] This advantage is however offset by the inflammation that sometimes results from clinical application of these metals.

As an alternative, solid lipid nanoparticles (SLNs) of 50 - 200 nm diameter are favored by their biocompatibility, biodegradability and the low cost of their surfactant molecule components.[8-10] Neutral Gd(acac) has been incorporated in the SLN hydrophobic core for use in neutron capture therapy of the brain.[11] In related work SLNs have been explored as containers and structural supports for imaging agents. In particular, several research groups have shown interest in Gd containing SLNs as MRI contrast agents. In an early report Aimé and coworkers described particles containing $[GdDTPA]^{2-}$ and $[GdDOTA]^{-}$.[12] Several later reports described SLNs with $[GdDTPA]^{-}$ on the particle surface or incorporated within the core.[13-18] In another approach $[GdDTPA]^{2-}$ anions have been assembled by charge pairing with a cationic SLN surface.[19]

The confinement of complexes to the SLN surface favors water exchange which is key to contrast enhancement in Gd-based T1 MRI contrast agents. We have designed a new approach to the formation of such agents by assembling modified LnDOTA complexes on an SLN surface and then crosslinking them to form a hyperbranched enclosure for the SLN. In this approach an SLN is encapsulated in a polyanionic network of ligands paired with surfactant counterions. Specifically, the monomer is the anionic complex, [Ln(DOTA-N,N',N'', N'''-tetrahomoserine)]$^-$ ([LnDhS]$^-$), (Ln = Eu, Gd) that is charge-paired with the cationic surfactant cetyltrimethylammonium (CTA^+) whose hydrophibic tail is associated with the SLN surface. The CTA^+ serves both to stabilize the SLN[20-23] and to form a double layer with the anionic complex. The DhS ligand has four hydroxyethyl groups at the α-carbons of the DOTA carboxymethyl group. The hydroxyl end groups serve as reaction sites for crosslinking by divinylsulfone (DVS).[24-25] The synthetic approach reported here is unique in its incorporation of [LnDhS]$^-$ as a monoanionic counterion to CTA^+, and as a monomeric precursor to a hyperbranched shell. (Figure 1)

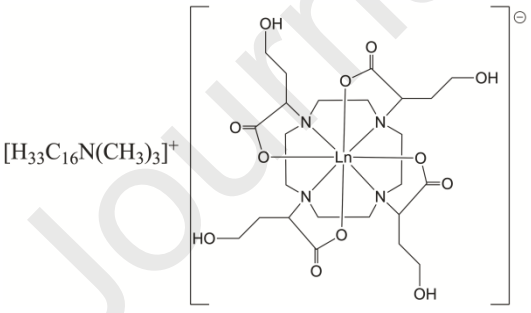

Figure 1: CTA^+[Eu(DOTA-N,N',N'', N'''-tetrahomoserine)]-, CTA[LnDhS], (Ln = Eu, Gd).

This is the first report of a crosslinked shell formation around an SLN template.[26] A preliminary examination of the crosslinked system with coordinated gadolinium shows an enhancement in relaxivity relative to small precursor gadolinium complexes.

2. Materials and methods

2.1 Materials

Emulsifying wax (EW) was obtained from Spectrum Chemicals. Polysorbate surfactant (Brij™ L23), and α-bromo-γ-butyrolactone were purchased from Sigma Aldrich Chemicals. Europium trichloride hexahydrate, gadolinium trichloride hexahydrate, divinyl sulfone (DVS) and potassium carbonate were purchased from Alfa Aesar Chemicals. Cetyltrimethylammonium chloride (CTA-Cl) was obtained from TCI America. All reagents were used as received.

2.2 Syntheses

2.2.1 Cyclen tetrabutyrolactone

Cyclen (1.00 g, 5.80 mmol), potassium carbonate (4.00 g, 29.02 mmol) and α-bromo-γ-butyrolactone (6.03 g, 36.57 mmol) were refluxed for 3 days in CH_3CN. The filtrate was collected and the solvent was removed by rotary evaporation. A solid product was collected after several ether-wash/centrifugation cycles. The solid was re-dissolved in 15 mL of chloroform and extracted twice with 5 mL of water. The chloroform solution was dried with

magnesium sulfate and the solvent was removed by rotary evaporation to give a yellow oil. After the addition of diethyl ether the product was deposited as a yellow powder in 71 % yield. ^{1}H NMR (400 MHz, $CDCl_3$, d): 4.45-4.25 (m, 8 H, O-CH_2), 3.95 (m, 4 H, N-CH), 3.70-3.49 (m, 4 H, cyclen-CH_2), 2.70-2.22 (m, 12 H, cyclen-CH_2), 2.40-2.25 (m, 8 H, lactone-CH_2); ^{13}C NMR (400 MHz, $CDCl_3$, d): 178.5 (C=O), 65.18 (O-CH_2), 59.90 (N-CH), 47.22 (cyclen-CH_2), 21.25 (lactone-CH_2). ESI-MS m/z: 508.9 $[M + H]^+$, 531.9 $[M + Na]^+$, 546.9 $[M + K]^+$.

2.2.2 CTAOH

CTA-Cl was stirred with KOH in anhydrous ethanol to prepare a stock solution of ethanolic cetyltrimethylammonium hydroxide (CTA-OH). The byproduct, KCl(s), was removed by filtration. The product was stored as a 1 M stock solution in ethanol.

2.2.3 CTA[EuDOTA(N,N',N'',N'''-tetra-α-homoserine)] (CTA[EuDhS])

Cyclen tetrabutyrolactone (0.13 g, 0.26 mmol) and cetyltrimethylammonium hydroxide (CTA-OH) (1.6 mmol) were combined in 10 mL of ethanol and stirred overnight butyrolactone ring opening to form DOTA-tetra-α-homoserine (DhS). Ethanol was removed by rotary evaporation and the product $(CTA)_4$DhS was re-dissolved in 20 mL of methanol followed by $EuCl_3.6H_2O$ (0.105 gm, 0.29 mmol). The solution was stirred for 3 hours, taken to dryness by rotary evaporation, dissolved in 25 mL of ethanol and refluxed for 1 hour. The solid product, CTA[EuDhS], was isolated by bench top centrifugation, and dried under vacuum to give 0.032 g of product, 12% yield. ^{1}H NMR (400 MHz, D_2O, d): 41.9 (s, 4H, ring CH axial, minor isomer),

22.0 (s, 4H, ring CH axial, major isomer). 8.1 (s, 1H, ring CH axial major isomer), 4.1 (s, 4H, α-CH (homoserine side chain)), 3.48 (m, 2H, α-N-CH_2 (CTA)), 3.0 (s, 9H, CH_3 (N-CH_3 from CTA), 1.6 (s, 2H, β-N-CH_2 (CTA)), 1.2-1.0 (d, 26H, -CH_2- (CTA backbone)), 0.79 (m, 3H, -CH_3 (CTA terminal methyl group)), -0.5 (s, 8H, β-CH (homoserine side chain)), -1.1 (s, 4H, γ-CH (homoserine side chain)), -2.0 (s, 4H, γ-CH (homoserine side chain)), -3.1 (s, 4H, ring CH equatorial, major isomer), -4.2 (s, 4 H, ring CH axial, major isomer), -4.9 (s, 4 H, ring CH equatorial, minor isomer), -8.6 (s, 4 H, ring CH equatorial, major isomer), -12.1 (s, 4 H, CH), -25.4 (s, 4 H, CH-minor isomer). ESI-MS m/z: 729.0 $[M]^-$.

2.2.4 CTA[GdDOTA(N,N',N''',N''''-tetra-a-homoserine)] (CTA[Gd(DhS)])

The product, CTA[Gd(DhS)], was obtained by the method above, but with $GdCl_3.6H_2O$ (0.29 mmol) substituted for $EuCl_3.6H_2O$. ESI-MS m/z: 734.3 $[M]^-$.

2.2.5 Formation of [EuDhS]SLN using Brij® L23

Solid lipid nanoparticles (SLNs) were prepared in an o/w microemulsion following the methods of Oyewumi and Mumper.[27] Briefly, emulsifying wax, 4 mg in 60 μL of chloroform, was deposited in a glass vial by evaporating the chloroform under a flow of nitrogen. The wax was then melted at 55 °C and maintained at that temperature while 1 mL of distilled water was added dropwise while stirring the emulsion at 1500 rpm. A homogenous milky slurry was formed and 60 μL (6 μmol) of Brij® L23 ($C_{12}H_{25}(OC_2H_4)_sOH$) solution (0.1 M stock soln.) were added. After 2 min, 1200 μL (60 μmol) of $CTA^+[Eu(DOTA)(N,N',N''',N''''$-tetra-a-homoserine)$]^-$ solution (50 mM stock soln.) were added. The solution was stirred until it became clear (about

30 min) and was then quickly cooled on an ice bath to form SLNs. The resulting SLN colloidal solution was diluted by the addition of 1 mL of cold water at 4 °C, filtered through a 0.22 μ pore size nylon membrane to remove large particles and stored at 4 °C.

2.2.6 Formation of $[EuDhS]_{CL}$SLN

The pH of the [EuDhS]SLN (aq) colloidal solution was adjusted to 12.0 by the dropwise addition of 1.0 M NaOH. The $[EuDhS]^-$ complexes were then polymerized by the slow addition of 25μL divinylsulfone (DVS), (4.2 equivalents). The solution was stirred for 3-6 hours after which the pH was lowered to 7.5-8 by the slow addition of 1.0 M HCl. Samples were stored as aqueous colloidal solutions at 4°C and remained transparent for more than 8 weeks.

2.3 Characterization

Proton NMR data, including relaxivity measurements, were obtained on a Bruker Advance 400 MHz NMR spectrometer. T1 relaxation measurements were carried out in deionized water (H_2O) solutions at 25º C with the temperature controlled by a BVT-3200. The aqueous (H_2O) samples were loaded into the internal capillary tubes of a coaxial cell with D_2O lock solvent in the exterior (5 mm o.d.) chamber. Acquisition parameters were: time domain 16K complex data point; 6410.26 Hz sweep width; 90º pulse with a length of 9 μs; repetition time T_R of 45 s; variable inversion time delay (τ) ranging from 100 ms to 5 s. T2 relaxation time was determined using a multi-echo Carr-Purcell-Meiboom-Gill (CPMG) sequence. Relaxivities r_1 and r_2 (mM^{-1} s^{-1}) were calculated from data collected at 5 different contrast agent concentrations based on the respective slopes of linear regressions generated from plots of the measured relaxation rates

(in seconds) versus the concentration of Gd^{3+} (in mM). Spectra were processed with XWIN-NMR version 3.5.6 to obtain relaxation curves.

Electrospray ionization (ESI) mass spectrometric data were obtained using an Agilent 1100 Series Capillary LCMSD Trap XCT MS spectrometer. Inductively coupled plasma optical emission spectroscopy (ICP-OES) chemical analyses were carried out by Galbraith Laboratories. TEM images were acquired on a Philips CM-12 electron microscope. Samples were prepared on carbon coated copper grids and the micrographs were recorded on a Gatan 1k x 1k digital camera. Fluorescence data was collected on a Hitachi F-2500 fluorescence spectrophotometer. All sample concentrations were at 10.8 mg/ml. Dynamic light scattering measurements were carried out on a Brookhaven Instruments ZetaPALS/Zeta Potential Analyzer and a Beckman-Coulter N4 Plus instrument.

3. Results and Discussion

3.1 Ligand synthesis and shell formation

In the synthesis of DOTA-tetrahomoserine (DhS) four equivalents of racemic bromobutyrolactone were added to tetraazacyclododecane (cyclen) in refluxing CH_3CN with K_2CO_3 to form tetraazacyclododecane-N,N',N'',N'''-tetrabutyrolactone. The reaction conditions were essentially the same as those reported in the synthesis of triazacyclononane N,N'N''-tributyrolactone.[28] Lactone ring-opening by base hydrolysis with CTA-OH gave a diastereomeric cyclic octadentate DOTA-tetrahomoserine derivative. Europium trichloride hexahydrate, $EuCl_3 \cdot 6H_2O$ was added to form the complex $[EuDhS]^-$. In the formation and workup of the complex, three equivalents of CTA-Cl and excess CTA-OH were removed,

leaving the salt, $CTA^+[EuDhS]^-$. The four pendant hydroxyethyl groups of the ligand were later employed to form a hyperbranched poly "EuDOTA" shell. (Figure 2)

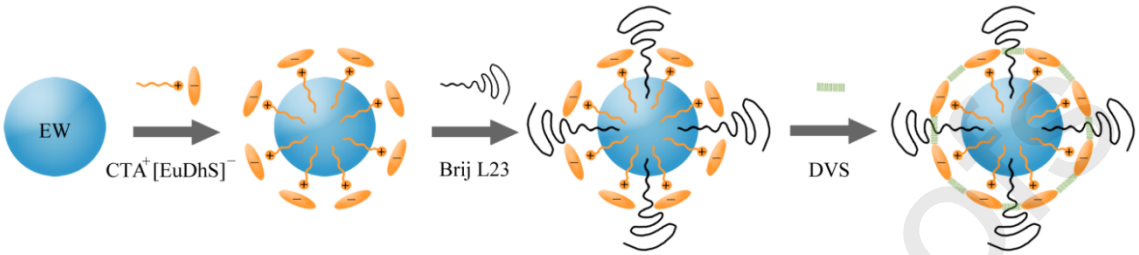

Figure 2. Schematic illustration of $CTA[EuDhS]_{CL}SLN$ formation where EW denotes the emulsifying wax core, and DVS denotes divinylsulfone.

The lipid core of the core shell NP is emulsifying wax (EW), a multicomponent matrix that consists of cetylstearyl alcohol and polysorbate 60 (USP28–Page 3107).[29] Emulsifying wax NPs have an amorphous matrix.[30] Following the methods of Oyewumi and Mumper, EW NPs were formed at 55 °C in an o/w microemulsion stabilized by the surfactants Brij L23 and the CTA^+ ion component of the CTA[EuDhS] salt.[27] With rapid cooling from 55 °C to 4 °C the molten wax solidified to yield an SLN that incorporates the lipophilic cationic tetraalkyl ammonium groups of CTA^+ but not the Eu complex counterion, $[EuDhS]^-$. The combined use of Brij L23 and CTA^+ ion surfactants draws on the work of Gao *et al.* who described the formation of stable CTA^+Br^-/Brij 35 mixed micelles.[31]

We surmised that the lipophilic tails of CTA^+ ($-C_{16}H_{33}$) and Brij L23 ($-C_{12}H_{25}$) would be embedded in the solid lipid matrix emulsifying wax, leaving the cationic headgroup of CTA^+ and the polyoxomer block of Brij L23 exposed to the aqueous bulk phase. The counterion

monomer, [EuDhS]$^-$, would then occupy the Stern layer as a mobile species that exchanges between fixed-position cationic CTA$^+$ headgroups anchored to the SLN surface with the construct represented by the formula (CTA[EuDhS]SLN). Mass action by small ions, such as Cl$^-$ in high salt solutions, can displace anionic [EuDhS]$^-$ complexes from the SLN surface. To prevent such displacement the [EuDhS]$^-$ assembly was stabilized by crosslinking at room temperature with divinyl sulfone[24] to form an anionic hyperbranched polymer shell enclosing the SLN. The core-shell NP surface of (CTA)[EuDhS]$_{CL}$SLN is represented in Figure 3. Adjacent particles are sterically shielded by the polyether -$(C_2H_4O)_{23}$-OH chains of Brij L23, which prevents inter-particle crosslinking.

Further crosslinking of [EuDhS]$^-$ to the lipid components cetylstearyl alcohol and polysorbate 60 of the SLN core is likely because a portion of the hydroxyl groups of these emulsifying wax components occupy the SLN surface.[32]

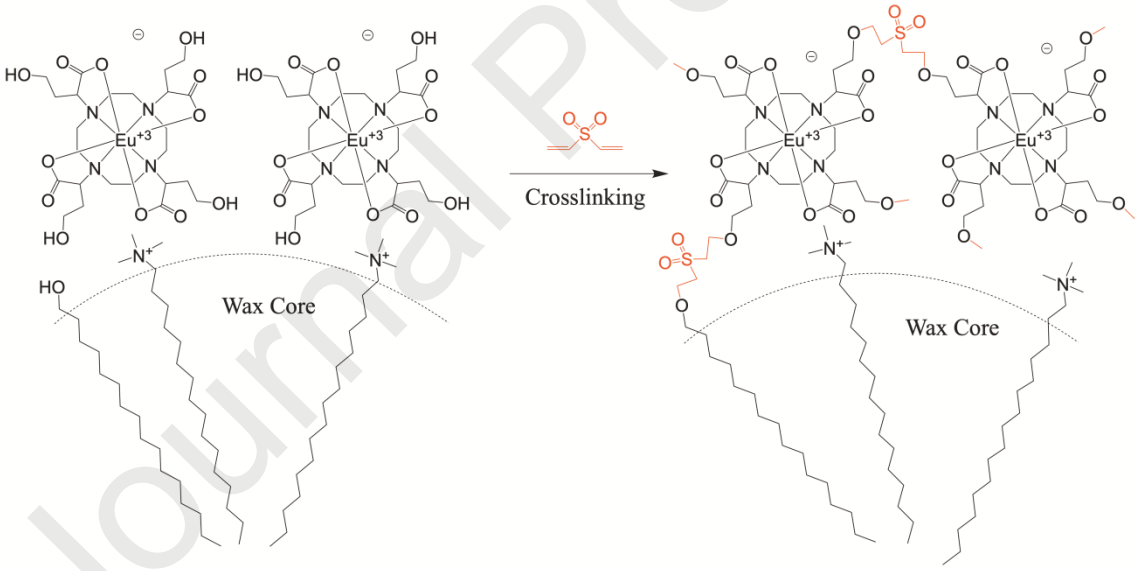

Figure 3. Proposed model of divinyl sulfone crosslinking of [EuDhS]$^-$ counterions and SLN surface hydroxyls in the Stern layer formed by [EuDhS]$^-$ and cations located on the SLN surface.

In the absence of crosslinking, samples of the nanoparticle CTA[EuDhS]SLN stored at 4 ^{o}C in aqueous media became turbid in about 2 weeks. By contrast, DVS crosslinking to form the

hybrid particle (CTA)[EuDhS]$_{CL}$SLN stabilized the particles against core disintegration, with no turbidity observed over a period of 8 weeks at 4 ^{o}C

3.2 Nanoparticle characterization

Dynamic light scattering measurements gave an average hydrodynamic diameter of 65.1 ± 7.3 nm for (CTA)[EuDhS]$_{CL}$SLN. The zeta potential of the crosslinked particle was +10.7 mV as measured by Doppler shift light scattering at pH 7.0. The particles were polydisperse by transmission electron microscopy, but were most abundant in the 50 nm range and with nearly spherical geometry. Smaller spherical particles were observed with diameters in the 5 – 10 nm range while a small fraction of larger particles appeared with diameters in the range of 100 nm. (Figure 4) Polydispersity is a common characteristic of SLNs.

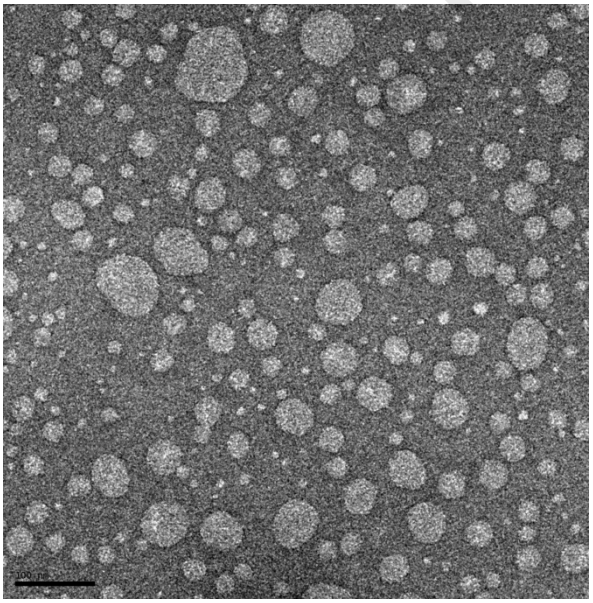

Figure 4. TEM image of SLN particles. (Bar represents 100 nm)

Europium in (CTA)[EuDhS]$_{CL}$SLN was found at the level of 5.58% of the particle mass by ICP-OES analysis. The average particle mass is determined based on particle size and the known density of emulsifying wax, which was assumed to apply to the particles in this investigation. The particle consists initially of emulsifying wax (EW), Brij L23, and (CTA)[EuDhS], and divinyl sulfone. However, over time, the mass ratios of these components undoubtedly change with the uptake of water and the loss of cetylstearyl alcohol and polysorbate 60 during the process of dialysis to remove excess non-incorporated molecules. Therefore we could only estimate the number of Eu ions per particle. Assuming a particle density of 0.85 g/cm^3, the same as bulk emulsifying wax at room temperature, a particle of 65.1 nm in diameter would have a mass of 1.22 x 10^{-16} g. The mass of Eu^{3+} per particle would then be 6.81 x 10^{-18} g, which corresponds to 2.70 x 10^4 Eu ions per particle. The number of lanthanide ions per particle is comparable to that reported for the well-known perfluorocarbon particles of equal diameter.[33]

3.3 Europium fluorescence

The crosslink stabilization of the capsule, [EuDhS]$^-_{CL}$, was investigated by fluorescence spectroscopy using 319 nm excitation that generated fluorescence with maxima at 578, 592 and 617 nm. Concurrent emission at 406 nm belongs to the EW core and was ignored. To probe the stability of the non-crosslinked (CTA)[EuDhS]SLN assembly, the sample was dialyzed (2.0 kDa cutoff dialysis membrane) against approximately 50 mL of 0.68 M sodium chloride, a 2000-fold excess of salt. The control for this experiment entailed the dialysis of the same system against distilled water. After 24 h the 617 nm europium emission peak of the uncrosslinked

(CTA)[EuDhS]SLN sample had decreased by 94%, while the fluorescence spectrum of the control was unchanged. (Figure 5A) The loss of fluorescence intensity was indicative of the Cl^- induced displacement of anionic $[EuDhS]^-$ complexes from the [EuDhS]SLN surface.

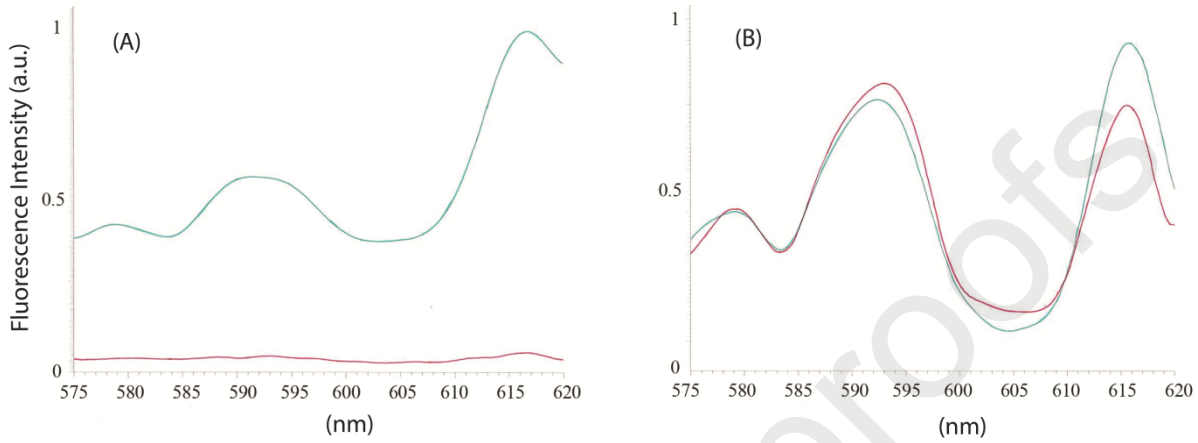

Figure 5. Fluorescence spectra in water of (A) NaCl-treated [EuDhS]SLN (red), salt-free control [EuDhS]SLN (green), (B) NaCl-treated crosslinked $[EuDhS]_{CL}$SLN (red) and the salt-free control $[EuDhS]_{CL}$SLN (green).

In the crosslinked sample, (CTA)$[EuDhS]_{CL}$SLN, it appears that at most 19% of the $[EuDhS]^-$ complexes were displaced by Cl^- as evidenced by the fluorescence intensity decrease at 617 nm.(Figure 5B) These results are consistent with the location of Eu complexes within the Stern and double layer regions of the SLN and highlight the efficacy of crosslinking $[EuDhS]^-$ to form a stable shell around the cationic SLN core.

The concentration of Eu complexes in the solid lipid core must be negligible because Eu fluorescence is absent after the displacement of Stern layer $[EuDhS]^-$ by Cl^- ions. This assessment, regarding the location of the Eu complex, is supported by a report that europium complexes exhibit fluorescence of comparable intensity both in solution and in sol-gel derived materials.[34] We therefore believe that if significant amounts of $[EuDhS]^-$ were located within

the SLN matrix the particle core would be fluorescent, which is not observed when $EuDhS^-$ is displaced by dialysis.

3.4 NMR analyses and gadolinium relaxivity

NMR analysis of (CTA)$[EuDhS]_{CL}$SLN is enhanced by the magnetic properties of europium that derive from low-lying states with $J > 0$ just above the diamagnetic $^7F_0$ ground state. The result is that the Eu^{3+} ion serves as an intrinsic shift reagent. The expected dipolar shifts of cyclen protons appear as a series of peaks in the upfield 0 – (-27) ppm region, and two peaks approximately 21 and 42 ppm downfield as referenced to the adventitious water peak at 4.7 ppm in D_2O.(Figure 6)

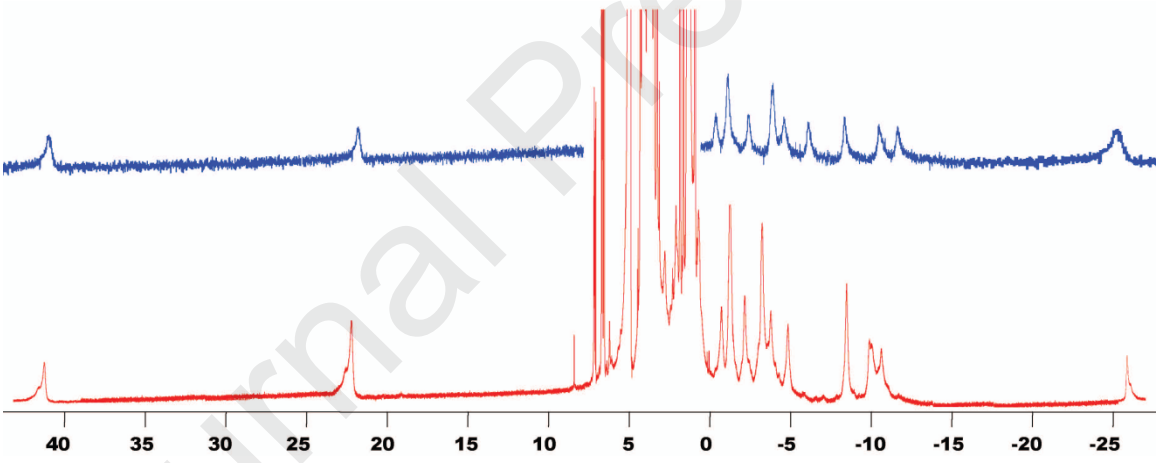

Figure 6. Proton NMR spectrum of CTA$[EuDhS]_{CL}$SLN in D_2O (bottom); K[EuDhS] in D_2O (top)**.**

The dipolar shift peaks of the shell-localized europium complexes of $[EuDhS]_{CL}$SLN are congruent with those of free $[EuDhS]^-$ and to a lesser extent with $[EuDOTA]^-$.[35-38] Peaks in the 0 – 7 ppm downfield region are assigned to the homoserine sidechain, crosslinkers and SLN core protons. The data from $[EuDhS]^-$ ions are complex because of structural isomerization, and

overlapping peaks from the diasteriomers δδδδ, δλλλ, δδλλ and δλδλ.[38] For this reason, the detailed assignment of peaks was not undertaken.

The congeners $[GdDhS]^-$ and $[GdDhS]_{CL}SLN$ were prepared from the product of $GdCl_3{\cdot}6H_2O$ and DhS^{4-}. The relaxivities of the $Gd[DhS]^-$ and $Gd[DhS]_{CL}SLN$, presented here as preliminary data, were found to be 4.16 and 7.70 $s^{-1}mM^{-1}$ respectively for r_1, and 5.43 and 11.58 respectively for r_2, with all data collected by NMR at 9.4 T (400 MHz) and 25°C.(Table 1) For $Gd[DhS]^-$ and $Gd[DhS]_{CL}SLN$ the respective r_2/r_1 ratios, 1.31 and 1.50, are comparable to the value of 1.5 reported for $Gd[DTPA]^-$ at 400 MHz.[6, 39-42] Further, the r_1 values for $Gd[DhS]^-$ and $Gd[DhS]_{CL}SLN$ are close to the high field (9.4 T) 4.25 – 5.16 mM^{-1} s^{-1} values reported by Li and coworkers for Gd(DO3A) tethered to a series of branched polymeric nanoparticles.[43] Based on the number of metal ion binding sites per particle, estimated from ICP-OES, the whole-particle relaxivities of $Gd[DhS]_{CL}SLN$ are r_1 = 1.39 x 10^5 $s^{-1}mM^{-1}$ (1.89 x 10^{-3} s^{-1} $mg^{-1}L$) and r_2 = 2.08 x 10^5 $s^{-1}mM^{-1}$ (2.83 x 10^{-3} s^{-1} $mg^{-1}L$). These values must be considered as averages because of the polydispersity of the SLN particles.

At low fields the per-Gd r_1 relaxivity for Gd complexes tethered to nanoscale structures is usually higher than those of simple Gd complexes in solution. This phenomenon has been explained by an increase in the rotational correlation time, τ_R, for macromolecular and nanoscale species.[44] However this advantage is lost at high field, typically above 1.5 T, where r_1 values tend to decrease and r_2 values can increase by as much as a factor of ten for Gd^{3+} complexes that bind rigidly to proteins.[45] The proximity of r_1 values for $Gd[DhS]_{CL}SLN$ and freely rotating $[GdDhS]^-$ complexes is consistent with the decoupling of the internal motion of crosslinked GdDhS groups from the slow rotation of the SLN core or hyperbranched DhS network that encloses the SLN. The *higher* r_1 relaxivity of $Gd[DhS]_{CL}SLN$ could plausibly be

attributed to faster water exchange in the crosslinked structure due to decreased hydrogen bonding after hydroxyl groups of DhS are removed by ligand cross linking.

Table 1. Relaxivity (r_1 and r_2) per Gd, or per particle in H_2O at 9.4 T (400MHz), 25°C

Compound		**Relaxivity (r_1, $s^{-1}mM^{-1}$)**	**Relaxivity (r_2, $s^{-1}mM^{-1}$)**
$Gd[DTPA]^{2-}$		4.6[a]	6.8[a]
$Gd[DhS]^{-}$		4.16	5.43
$Gd[DhS]_{CL}SLN$		7.70	11.58
$Gd[DhS]_{CL}SLN$	$2.70x10^4$ (complexes per particle)	$2.08x10^5$ [b] (per particle)	$3.13x10^5$ [b] (per particle)

[a] References:[6, 39-42].

[b] Relaxivity per particle is estimated from the Gd^{3+} population on the particle surface.

In the early work by Morel *et al.* gadolinium complexes associated with solid lipid NPs had r_1 relaxivities that were similarly comparable to small freely rotating gadolinium complexes.[12] Results from more recent studies suggest that r_1 relaxivity values $\geq 4 - 5$ s^{-1} mM^{-1} derive only from surface localized Gd complexes. Clues about relaxivity and structure in nanoparticulate gadolinium-based MRI contrast agents come from liposomal agents where the relaxivity for the inner interface is apparently diminished by the low rate of water exchange between the inner and outer regions.[46] In these agents GdDTPA and GdDOTA complexes are preferentially attached to the outer layer of the liposomal bilayer.[47] It therefore appears that maximal relaxivity in NP agents requires that GdDTPA and GdDOTA complexes be fully exposed to *bulk* water. Our system fulfills this requirement. Furthermore, GdDOTA is favored as a contrast agent by its high stability constant and inertness to substitution by metal ions that are endogenous to the physiological environment.[48-49] It is reasonable to assume that crosslinked DhS retains kinetic

and thermodynamic parity with the free DOTA ligand. With refinement to attain monodispersity, $[LnDhS]_{CL}$SLN could be considered for colonography where absorption into the bloodstream and slow clearance through the liver is not a factor.[16] Similar systems with cleavable ester linkages might prove acceptable for broader applications.

4. Conclusions

Several reports have described the use of SLNs for MRI contrast enhancement.[12-13, 16-19] For those systems the location of the Gd^{3+} coordinating groups were not a focus of the study. The work described here highlights the *spatial* distribution of $[EuDhS]_{CL}$ relative to the SLN core, with a preliminary look at the related relaxivity of the $[GdDhS]_{CL}$ units of the $[LnDhS]_{CL}$SLN system.

We employed CTA^+ to electrostatically position counterion anionic complexes, $[Ln(DhS)]^-$, to form a shell around the cationic surface of the SLN core. These anionic complex monomers are homoserine derivatives of $[LnDOTA]^-$ (Ln = Eu^{3+} and Gd^{3+}) with pendant hydroxyl groups that are crosslinked by DVS to produce a hyperbranched polymer shell around an SLN core. Fluorescence data show that anionic $[LnDhS]^-$ complexes are not incorporated in the SLN core but instead are restricted to the Stern layer at the cationic surface of the SLN.

The nanoparticulate $[LnDhS]_{CL}$SLN system described here illustrates a convenient route to assemble an organic nanoparticulate contrast agent consisting of anionic LnDOTA-tetrahomoserine, [LnDhS], monomers assembled as a crosslinked capsule, $[LnDhS]_{CL}$, that encloses the cationic surface of an SLN. Preliminary measurements show the r_1 relaxivity value

of $[Gd(DhS)]^-$ in the shell of $(CTA)[Gd(DhS)]_{CL}SLN$, to be 7.70 $s^{-1}mM^{-1}$, which could be suitable for certain clinical imaging applications.

Acknowledgements

We thank Dr. Zahi A. Fayad and Ms. Jojo Read and Dr. Iwao Teraoka for assistance in the acquisition of dynamic light scattering data. This work was supported by the National Science Foundation Chemistry Research Instrumentation and Facilities program (Grant CHE-0840277), and the NYU Research Challenge Fund.

Abbreviations: CTA - cetyltrimethylammonium
DhS - DOTA-tetrahomoserine
DOTA - 1,4,7,10-tetraazacyclododecane-1,4,7,10-tetraacetate
DTPA - diethylenetriaminepentaacetic acid
DVS - divinylsulfone
EW - emulsifying wax
SLN - solid lipid nanoparticle

References

1. Na, H. B.; Hyeon, T., Nanostructured T1 MRI contrast agents. *J. Mater. Chem.* **2009,** *19* (35), 6267-6273.
2. Wallace, K. D.; Hughes, M. S.; Marsh, J. N.; Caruthers, S. D.; Lanza, G. M.; Wickline, S. A. In *From in vivo ultrasound and MRI imaging to therapy: contrast agents based on target-specific nanoparticles*, Wiley-VCH Verlag GmbH & Co. KGaA: 2009; pp 19-50.
3. Accardo, A.; Tesauro, D.; Aloj, L.; Pedone, C.; Morelli, G., Supramolecular aggregates containing lipophilic Gd(III) complexes as contrast agents in MRI. *Coord. Chem. Rev.* **2009,** *253* (Copyright (C) 2013 American Chemical Society (ACS). All Rights Reserved.), 2193-2213.
4. Aime, S.; Delli, C. D.; Geninatti, C. S.; Gianolio, E.; Terreno, E., Pushing the Sensitivity Envelope of Lanthanide-Based Magnetic Resonance Imaging (MRI) Contrast Agents for Molecular Imaging Applications. *Acc. Chem. Res.* **2009,** *42* (Copyright (C) 2013 American Chemical Society (ACS). All Rights Reserved.), 822-831.
5. Walters, M., The Exploration of Biomedical Multimodality in Small Solid Core Nanoparticles. In *Hybrid Nanomaterials: Synthesis, Characterization, and Applications*, Interscience Book ed.; Chauhan, B. P. S., Ed. Wiley: 2011; p 300.
6. Siddiqui, T. S.; Jani, A.; Williams, F.; Muller, R. N.; Elst, L.; Laurent, S.; Yao, F.; Wadghiri, Y. Z.; Walters, M. A., Lanthanide complexes on Ag nanoparticles: Designing contrast agents for magnetic resonance imaging. *J. Colloid Interface Sci.* **2009,** *337* (1), 88-96.

7. Vigderman, L.; Zubarev, E. R., Therapeutic platforms based on gold nanoparticles and their covalent conjugates with drug molecules. *Adv. Drug Delivery Rev.* **2013,** *65* (Copyright (C) 2013 American Chemical Society (ACS). All Rights Reserved.), 663-676.
8. Lammers, T.; Aimé, S.; Hennink, W. E.; Storm, G.; Kiessling, F., Theranostic Nanomedicines. *Acc. Chem. Res.* **2011,** *44* (10), 1029-1038.
9. Andreozzi, E.; Seo, J. W.; Ferrara, K.; Louie, A., Novel method to label solid lipid nanoparticles with 64Cu for positron emission tomography imaging. *Bioconjugate Chemistry* **2011,** *22* (4), 808-818.
10. Müller, R. H.; Mader, K.; Gohla, S., Solid lipid nanoparticles (SLN) for controlled drug delivery - a review of the state of the art. *Eur. J. Pharm. Biopharm.* **2000,** *50* (1), 161-177.
11. Oyewumi, M. O.; Mumper, R. J., Engineering tumor-targeted gadolinium hexanedione nanoparticles for potential application in neutron capture therapy. *Bioconjugate Chemistry* **2002,** *13* (6), 1328-1335.
12. Morel, S.; Terreno, E.; Ugazio, E.; Aimé, S.; Gasco, M. R., NMR relaxometric investigations of solid lipid nanoparticles (SLN) containing gadolinium(III) complexes. *Eur. J. Pharm. Biopharm.* **1998,** *45* (2), 157-163.
13. Zhu, D. H.; White, R. D.; Hardy, P. A.; Weerapreeyakul, N.; Sutthanut, K.; Jay, M., Biocompatible nanotemplate-engineered nanoparticles containing gadolinium: Stability and relaxivity of a potential MRI contrast agent. *J. Nanosci. Nanotechnol.* **2006,** *6* (4), 996-1003.
14. Zhu, D.; Lu, X. L.; Hardy, P. A.; Leggas, M.; Jay, M., Nanotemplate-engineered nanoparticles containing gadolinium for magnetic resonance imaging of tumors. *Investigative Radiology* **2008,** *43* (2), 129-140.
15. Bui, T.; Stevenson, J.; Hoekman, J.; Zhang, S. R.; Maravilla, K.; Ho, R. J. Y., Novel Gd Nanoparticles Enhance Vascular Contrast for High-Resolution Magnetic Resonance Imaging. *Plos One* **2010,** *5* (9).
16. Sun, J.; Zheng, W.; Zhang, H.; Wu, T.; Yuan, H.; Yang, X.; Zhang, S., Development of nanoparticle-based magnetic resonance colonography. *Magn Reson Med* **2011,** *65* (3), 673-9.
17. Rolla, G. A.; Botta, M.; Tei, L.; Cabella, C.; Ghiani, S.; Brioschi, C.; Maiocchi, A., Paramagnetic solid lipid nanoparticles as a novel platform for the development of molecular MRI probes. *Chemistry* **2013,** *19* (34), 11189-93.
18. Ghiani, S.; Capozza, M.; Cabella, C.; Coppo, A.; Miragoli, L.; Brioschi, C.; Bonafe, R.; Maiocchi, A., In vivo tumor targeting and biodistribution evaluation of paramagnetic solid lipid nanoparticles for magnetic resonance imaging. *Nanomedicine (N. Y., NY, U. S.)* **2017,** *13* (2), 693-700.
19. Chen, Z.-j.; Zhang, N., Preliminary study on cationic solid lipid nanoparticles/Gd-DTPA complex as molecular imaging agent. *Zhongguo Xinyao Zazhi* **2009,** *18* (15), 1443-1447.
20. Eccleston, G. M., Functions of mixed emulsifiers and emulsifying waxes in dermatological lotions and creams. *Colloid Surface A* **1997,** *123*, 169-182.
21. Kim, H. R.; Kim, I. K.; Bae, K. H.; Lee, S. H.; Lee, Y.; Park, T. G., Cationic solid lipid nanoparticles reconstituted from low density lipoprotein components for delivery of siRNA. *Mol. Pharmaceut.* **2008,** *5* (4), 622-631.
22. Tabatt, K.; Sameti, M.; Olbrich, C.; Muller, R. H.; Lehr, C. M., Effect of cationic lipid and matrix lipid composition on solid lipid nanoparticle-mediated gene transfer. *Eur. J. Pharm. Biopharm.* **2004,** *57* (2), 155-162.
23. Siddiqui, A.; Patwardhan, G. A.; Liu, Y. Y.; Nazzal, S., Mixed backbone antisense glucosylceramide synthase oligonucleotide (MBO-asGCS) loaded solid lipid nanoparticles: In vitro characterization and reversal of multidrug resistance in NCI/ADR-RES cells. *Int. J. Pharm.* **2010,** *400* (1-2), 251-259.

24. Liu, S. Y.; Ma, Y. H.; Armes, S. P., Direct verification of the core-shell structure of shell cross-linked micelles in the solid state using X-ray photoelectron spectroscopy. *Langmuir* **2002,** *18* (21), 7780-7784.
25. Read, E. S.; Armes, S. P., Recent advances in shell cross-linked micelles. *Chem. Comm.* **2007,** (29), 3021-3035.
26. Walters, M. A. Lanthanoid complex capsule and particle contrast agents, methods of making and using thereof. WO2012151539A2, 2012.
27. Oyewumi, M. O.; Mumper, R. J., Gadolinium-loaded nanoparticles engineered from microemulsion templates. *Drug Dev. Ind. Pharm.* **2002,** *28* (3), 317-328.
28. Lazar, I.; Egri, A.; Kiraly, R.; Baranyai, Z.; Ivanyi, T.; Brucher, E., Synthesis, conformation and equilibrium study of new piperazine and azamacrocyclic ligands with N-(tetrahydro-2-oxofuran-3-yl) and N-[(carboxy)(2-hydroxyethyl)methyl] pendant arms. *Eur. J. Org. Chem.* **2002,** (2), 351-360.
29. Dong, X.; Mumper, R. J., The metabolism of fatty alcohols in lipid nanoparticles by alcohol dehydrogenase. *Drug Dev. Ind. Pharm.* **2006,** *32* (8), 973-980.
30. Ulrich, A. S., Biophysical aspects of using liposomes as delivery vehicles. *Biosci. Rep.* **2002,** *22* (2), 129-150.
31. Gao, H. C.; Zhu, R. X.; Yang, X. Y.; Mao, S. Z.; Zhao, S.; Yu, J. Y.; Du, Y. R., Properties of polyethylene glycol(23) lauryl ether with cetyltrimethylammonium bromide in mixed aqueous solutions studied by self-diffusion coefficient NMR. *J. Colloid Interface Sci.* **2004,** *273* (2), 626-631.
32. Eccleston, G. M., Multiple-Phase Oil-in-Water Emulsions. *J Soc Cosmet Chem* **1990,** *41* (1), 1-22.
33. Tran, T. D.; Caruthers, S. D.; Hughes, M.; Marsh, J. N.; Cyrus, T.; Winter, P. M.; Neubauer, A. M.; Wickline, S. A.; Lanza, G. M., Clinical applications of perfluorocarbon nanoparticles for molecular imaging and targeted therapeutics. *Int. J. Nanomed.* **2007,** *2* (4), 515-526.
34. Matthews, L. R.; Knobbe, E. T., Luminescence Behavior of Europium Complexes in Sol-Gel Derived Host Materials. *Chem. Mater.* **1993,** *5* (12), 1697-1700.
35. Aimé, S.; Botta, M.; Fasano, M.; Marques, M. P. M.; Geraldes, C. F. G. C.; Pubanz, D.; Merbach, A. E., Conformational and coordination equilibria on DOTA complexes of lanthanide metal ions in aqueous solution studied by H-1-NMR spectroscopy. *Inorg. Chem.* **1997,** *36* (10), 2059-2068.
36. Desreux, J. F., Nuclear Magnetic-Resonance Spectroscopy of Lanthanide Complexes with a Tetraacetic Tetraaza Macrocycle - Unusual Conformation Properties. *Inorg. Chem.* **1980,** *19* (5), 1319-1324.
37. Aimé, S.; Botta, M.; Ermondi, G., Nmr-Study of Solution Structures and Dynamics of Lanthanide(Iii) Complexes of Dota. *Inorg. Chem.* **1992,** *31* (21), 4291-4299.
38. Woods, M.; Aime, S.; Botta, M.; Howard, J. A. K.; Moloney, J. M.; Navet, M.; Parker, D.; Port, M.; Rousseaux, O., Correlation of water exchange rate with isomeric composition in diastereoisomeric gadolinium complexes of tetra(carboxyethyl)dota and related macrocyclic ligands. *J. Am. Chem. Soc.* **2000,** *122* (40), 9781-9792.
39. Cage, B.; Russek, S. E.; Shoemaker, R.; Barker, A. J.; Stoldt, C.; Ramachandaran, V.; Dalal, N. S., The utility of the single-molecule magnet Fe-8 as a magnetic resonance imaging contrast agent over a broad range of concentration. *Polyhedron* **2007,** *26* (12), 2413-2419.
40. Nakamura, E.; Makino, K.; Okano, T.; Yamamoto, T.; Yokoyama, M., A polymeric micelle MRI contrast agent with changeable relaxivity. *J. Controlled Release* **2006,** *114* (3), 325-333.

41. Sun, G. Y.; Feng, J. H.; Jing, F. Y.; Pei, F. K.; Liu, M. L., Synthesis and evaluation of novel polysaccharide-Gd-DTPA compounds as contrast agent for MRI. *J. Magn. Magn. Mater.* **2003,** *265* (2), 123-129.
42. Vaccaro, M.; Accardo, A.; D'Errico, G.; Schillen, K.; Radulescu, A.; Tesauro, D.; Morelli, G.; Paduano, L., Peptides and gd complexes containing colloidal assemblies as tumor-specific contrast agents in MRI: Physicochemical characterization. *Biophys. J.* **2007,** *93* (5), 1736-1746.
43. Li, Y.; Laurent, S.; Esser, L.; Vander Elst, L.; Muller, R. N.; Lowe, A. B.; Boyer, C.; Davis, T. P., The precise molecular location of gadolinium atoms has a significant influence on the efficacy of nanoparticulate MRI positive contrast agents. *Polym. Chem.* **2014,** *5* (7), 2592-2601.
44. Caravan, P.; Ellison, J. J.; McMurry, T. J.; Lauffer, R. B., Gadolinium(III) Chelates as MRI Contrast Agents: Structure, Dynamics, and Applications. *Chem. Rev.* **1999,** *99* (9), 2293-2352.
45. Caravan, P.; Farrar, C. T.; Frullano, L.; Uppal, R., Influence of molecular parameters and increasing magnetic field strength on relaxivity of gadolinium- and manganese-based T1 contrast agents. *Contrast Media Mol Imaging* **2009,** *4* (2), 89-100.
46. Muller, R. N.; Laurent, S.; Elst, L. V.; Thirifays, C., Paramagnetic liposomes: Inner versus outer membrane relaxivity of DPPC liposomes incorporating lipophilic gadolinium complexes. *Langmuir* **2008,** *24* (8), 4347-4351.
47. Kamaly, N.; Miller, A. D., Paramagnetic Liposome Nanoparticles for Cellular and Tumour Imaging. *Int. J. Mol. Sci.* **2010,** *11* (4), 1759-1776.
48. Viola-Villegas, N.; Doyle, R. P., The coordination chemistry of 1,4,7,10-tetraazacyclododecane-N,N ',N ",N "'-tetraacetic acid (H(4)DOTA): Structural overview and analyses on structure-stability relationships. *Coord. Chem. Rev.* **2009,** *253* (13-14), 1906-1925.
49. Laurent, S.; Vander Elst, L.; Henoumont, C.; Muller, R. N., How to measure the transmetallation of a gadolinium complex. *Contrast Media & Molecular Imaging* **2010,** *5* (6), 305-308.

Author Statement File

The project described in the submitted manuscript was conceived by Prof. Walters. The initial monomer ligand syntheses were carried out by Eser Akturk, an undergraduate in the Walters group. After his graduation the syntheses were optimized by Joo-Hyung, a graduate student in the group. Sujeethraj Koppolu, another graduate student in the group, was responsible for nanoparticle formation. Lastly Eric Roth an electron microscopist played a pivotal role in particle characterization.

Declaration of interests

☒ The authors declare that they have no known competing financial interests or personal relationships that could have appeared to influence the work reported in this paper.

☐The authors declare the following financial interests/personal relationships which may be considered as potential competing interests:

- Anionic metal complexes are assembled with the aid of cationic surfactants
- The surfactant tails are embedded in a solid lipid nanoparticle core which serves to arrange the metal complexes above the nanoparticle surface
- The metal complexes are then crosslinked and the resulting hyperbranched metallopolymer network encloses the solid lipid nanoparticle
- The resulting nanoparticle containing gadolinium can, in principle, be used for certain types of high contrast MRI imaging where cell uptake is proscribed

Relaxivity of Gd(Dhs) complex

[Gd] (mM)	T_1 (s)	$1/T_1$ (s^{-1})	T_2 (s)	$1/T_2$ (s^{-1})
1	0.117298	8.525295	0.08774	11.39731
2	0.076783	13.02372	0.05842	17.11743
3	0.058906	16.9762	0.04375	22.85714
4	0.045826	21.82167	0.03457	28.92682
5	0.04028	24.82597	0.03039	32.90556

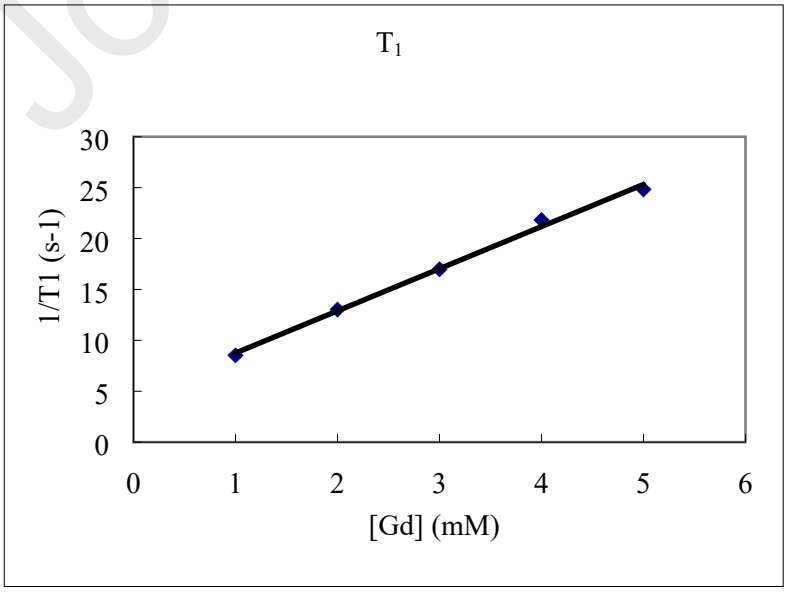

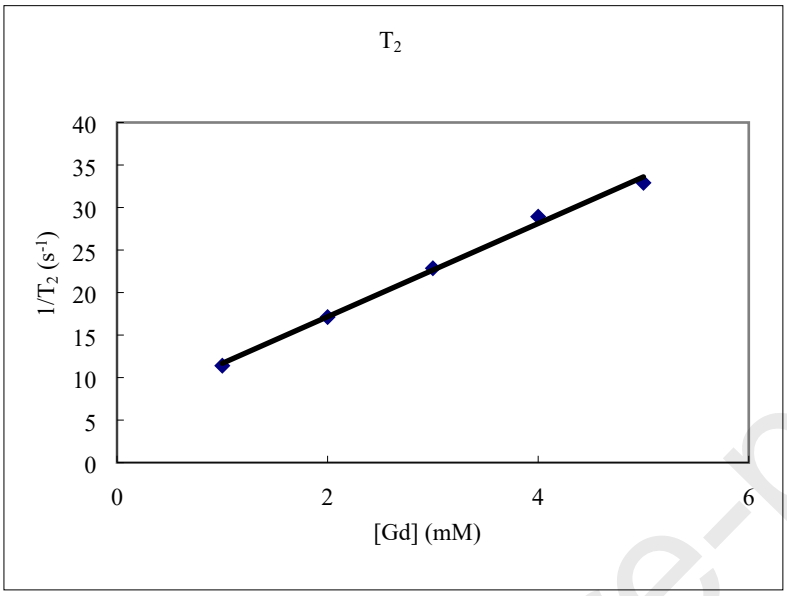

relaxivity of CTA[GdDhS)]$_{CL}$ SLN Final

sample #	[c] (mM)	T_1 (s)	$1/T_1$ (s^{-1})	[c] (mM)	T_2 (s)	$1/T_2$ (s^{-1})
1	4.38	0.026123	38.28044	3.83	0.020112	49.72156
2	1.46	0.065467	15.27487	1.276667	0.05279	18.94298
3	0.73	0.085826	11.65148	0.638333	0.06828	14.64558
4	0.365	0.149785	6.676236	0.319167	0.12146	8.233163
5	0.219	0.16753	5.96908	0.1915	0.13814	7.239033